

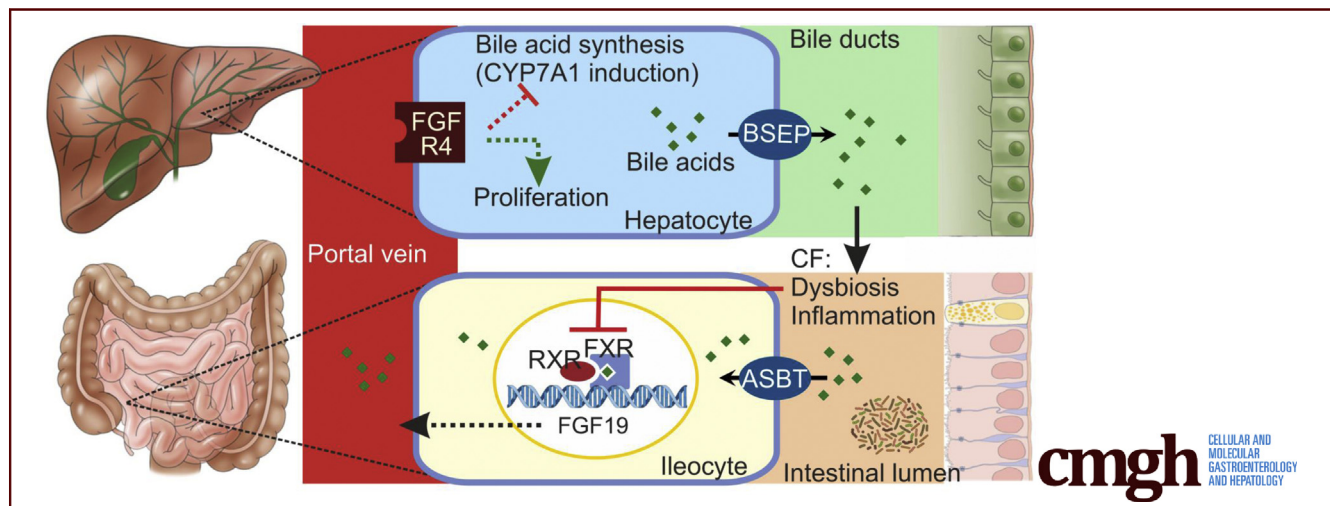
## ORIGINAL RESEARCH

## Impaired Intestinal Farnesoid X Receptor Signaling in Cystic Fibrosis Mice

Pauline T. Ikpa,<sup>1</sup> Marcela Doktorova,<sup>2</sup> Kelly F. Meijssen,<sup>1</sup> Natascha D. A. Nieuwenhuijze,<sup>1</sup> Henkjan J. Verkade,<sup>2</sup> Johan W. Jonker,<sup>2</sup> Hugo R. de Jonge,<sup>1</sup> and Marcel J. C. Bijvelds<sup>1</sup>

<sup>1</sup>Department of Gastroenterology and Hepatology, Erasmus MC University Medical Center, Rotterdam, The Netherlands;

<sup>2</sup>Section of Molecular Metabolism and Nutrition, Department of Pediatrics, University of Groningen, University Medical Center Groningen, Groningen, The Netherlands



## SUMMARY

In a cystic fibrosis mouse model, intestinal dysbiosis and inflammation repress signaling through the bile acid-activated nuclear receptor farnesoid X receptor. This repression impairs feedback regulation of hepatic bile acid synthesis and limits the capacity for homeostatic liver regeneration.

**BACKGROUND & AIMS:** The bile acid (BA)-activated farnesoid X receptor (FXR) controls hepatic BA synthesis and cell proliferation via the intestinal hormone fibroblast growth factor 19. Because cystic fibrosis (CF) is associated with intestinal dysbiosis, anomalous BA handling, and biliary cirrhosis, we investigated FXR signaling in CF.

**METHODS:** Intestinal and hepatic expression of FXR target genes and inflammation markers was assessed in *Cftr* null mice and controls. Localization of the apical sodium-dependent BA transporter was assessed, and BAs in gastrointestinal tissues were analyzed. The CF microbiota was characterized and FXR signaling was investigated in intestinal tissue and organoids.

**RESULTS:** Ileal murine fibroblast growth factor 19 ortholog (*Fgf15*) expression was strongly reduced in CF mice,

compared with controls. Luminal BA levels and localization of apical sodium-dependent BA transporter was not affected, and BAs induced *Fgf15* up to normal levels in CF ileum, ex vivo, and CF organoids. CF mice showed a dysbiosis that was associated with a marked up-regulation of genes involved in host-microbe interactions, including those involved in mucin glycosylation, antimicrobial defense, and Toll-like receptor signaling. Antibiotic treatment reversed the up-regulation of inflammatory markers and restored intestinal FXR signaling in CF mice. Conversely, FXR-dependent gene induction in ileal tissue and organoids was repressed by bacterial lipopolysaccharide and proinflammatory cytokines, respectively. Loss of intestinal FXR activity was associated with a markedly blunted hepatic trophic response to oral BA supplementation, and with impaired repression of *Cyp7a1*, the gene encoding the rate-limiting enzyme in BA synthesis.

**CONCLUSIONS:** In CF mice, the gut microbiota represses intestinal FXR activity, and, consequently, FXR-dependent hepatic cell proliferation and feedback control of BA synthesis. (*Cell Mol Gastroenterol Hepatol* 2019;■:■-■; <https://doi.org/10.1016/j.jcmgh.2019.08.006>)

**Keywords:** Bile Acids and Salts; Gut Microbiota; Fibroblast Growth Factors; Cytoplasmic and Nuclear Receptors.

**B**ile acids (BAs) are amphiphilic molecules synthesized from cholesterol in the liver. Upon release into the proximal small intestine, BAs aid the absorption of dietary lipids, after which they are reabsorbed, mainly through active uptake in the distal ileum via the apical sodium-dependent BA transporter (ASBT; encoded by SLC10A2).<sup>1</sup> Although very little of the load entering the intestine escapes re-uptake, small amounts of BA pass through the colon and are excreted in the feces. Fecal loss is compensated for by de novo synthesis, which is regulated through a finely tuned homeostatic control mechanism, to maintain a near-constant body BA pool. One of the key elements of this control mechanism is the activation of the farnesoid X receptor (FXR) in ileal epithelial cells by reclaimed BAs.<sup>2,3</sup> Intestinal FXR activation induces the expression of an array of genes involved in BA transport and metabolism. Most importantly, BA reabsorption triggers the production and release of fibroblast growth factor (FGF)19. This hormone, through activation of its hepatic receptor, represses expression of CYP7A1, the gene encoding the cholesterol 7 $\alpha$ -hydroxylase that catalyzes the rate-limiting step in cholic acid (CA) synthesis.<sup>4</sup> The importance of this feedback loop is underlined by the observation that in FGF15 (the murine FGF19 ortholog)-deficient mice, hepatic BA synthesis and intestinal delivery are stimulated to a level that exceeds the capacity for reabsorption, resulting in enhanced fecal excretion.<sup>5</sup> In addition, FGF15/19 has trophic effects in the liver, which are crucial for liver regeneration after injury.<sup>6,7</sup> Through its effects on hepatic BA synthesis, FGF15/19 signaling may prevent cholestasis-induced liver damage.<sup>8,9</sup>

Cystic fibrosis (CF), an autosomal-recessive disease caused by mutations in the CF transmembrane conductance regulator (*CFTR*) gene, is characterized by focal biliary cirrhosis, which in a subgroup of patients (approximately 30%) progresses to a clinically significant, advanced stage of CF-related liver disease (CFLD).<sup>10</sup> Principally, this cholangiopathy is thought to be caused by obstruction of the intrahepatic bile ducts by mucoid secretions and accumulation of hydrophobic BAs, but other factors, such as exposure to gut-derived endotoxins, also may contribute.<sup>10–12</sup> Bile of CF patients shows a relative increase in CA levels and a decrease in the levels of secondary BAs, which is indicative of enhanced de novo synthesis.<sup>13</sup> This also is implied by the observation that the body BA pool size of CF patients is normal to large, despite the fact that, in many CF patients, fecal BA excretion is abnormally high, whereas plasma FGF19 levels are low.<sup>13,14</sup> Fecal BA wasting, high biliary CA levels, and a mild cholangiopathy also have been observed in most CF mouse models.<sup>15–17</sup> These observations suggest that, perhaps because of interrupted enterohepatic cycling of BAs, the FXR/FGF19 signaling pathway is suppressed in CF. Indeed, strongly reduced ileal *Asbt* and *Fgf15* expression, indicative of reduced BA uptake and FXR activation, was reported for 1 CF mouse model.<sup>18</sup> In this instance, low FXR/FGF15 signaling was attributed to defective gallbladder emptying, which severely limited intestinal delivery of BAs. Furthermore, more circumstantial evidence for attenuated FXR/FGF15

signaling in CF was provided by one of our previous studies, in which it was shown that dietary CA supplementation, which is known to induce hepatocyte proliferation through an FXR-/FGF15-dependent pathway, triggers a markedly blunted response in CF mice.<sup>6,7,19</sup> Assuming that the virtual absence of this response in our CF mice is indeed linked to low intestinal FGF15 production, our data imply that enhanced intestinal delivery of BAs (as per diet) does not correct FXR/FGF15 signaling. This led us to speculate that, apart from defective gallbladder emptying, other factors may contribute to impaired FXR/FGF15 signaling.

In recent years it has become apparent that the gut microbiota, through modulation of intestinal FXR signaling, is a key regulator of BA metabolism. In mice, intraluminal microbial BA conversion appears to be a key determinant of BA uptake and FXR activity because both eradication of the microflora and colonization of the gut by probiotics were shown to repress *Fgf15* induction markedly.<sup>20–22</sup> Furthermore, it was shown that bacterial endotoxins eliciting an acute-phase response, repress hepatic FXR signaling, and that FGF15 production is reduced in inflamed intestinal tissue.<sup>23–26</sup> Because murine CF models show distinct quantitative and qualitative changes in the gut microbiota (dysbiosis) and inflammation of the gut wall, it is conceivable that BA biotransformation and/or exposure to endotoxins leads to a loss of FXR-dependent feedback control of hepatic BA synthesis.<sup>27–29</sup>

Presently, we have investigated the role of the gut microbiota in intestinal FXR signaling in CF mice. We show that intestinal FXR signaling is attenuated markedly in CF mice, despite normal luminal BA levels, and that repression of FXR signaling persists upon supraphysiological BA dosage, but that constraining bacterial colonization by antibiotic treatment reduces the expression of inflammation markers and normalizes *Fgf15* expression and BA synthesis.

## Results

### *Intestinal FXR Signaling Is Impaired in CF Mice*

The expression of FXR targets *Fgf15* and *Shp* (*Nr0b2*) was markedly lower in the ileum of CF mice compared with littermate controls, whereas expression of *Fxr* (*Nr1h4*) itself was similar between genotypes (Figure 1A). Congruent with low intestinal FGF15 production, hepatic expression of *Cyp7a1* was enhanced in CF mice, whereas the expression of the FGF15 receptor, *Fgfr4*, in the intestine and in the liver, was not affected.

**Abbreviations used in this paper:** ASBT, apical sodium-dependent bile acid transporter; BA, bile acid;  $\beta$ -MCA,  $\beta$ -muricholic acid; B4galt1,  $\beta$ -1,4-galactosyltransferase I; CA, cholic acid; CF, cystic fibrosis; CFLD, cystic fibrosis-related liver disease; CFTR, cystic fibrosis transmembrane conductance regulator; FGF, fibroblast growth factor; Fut2, fuc  $\alpha$ 1-2 fucosyltransferase; FXR, farnesoid X receptor; LPS, lipopolysaccharide; TLR, Toll-like receptor.

© 2019 The Authors. Published by Elsevier Inc. on behalf of the AGA Institute. This is an open access article under the CC BY-NC-ND license (<http://creativecommons.org/licenses/by-nc-nd/4.0/>).

2352-345X

<https://doi.org/10.1016/j.jcmgh.2019.08.006>

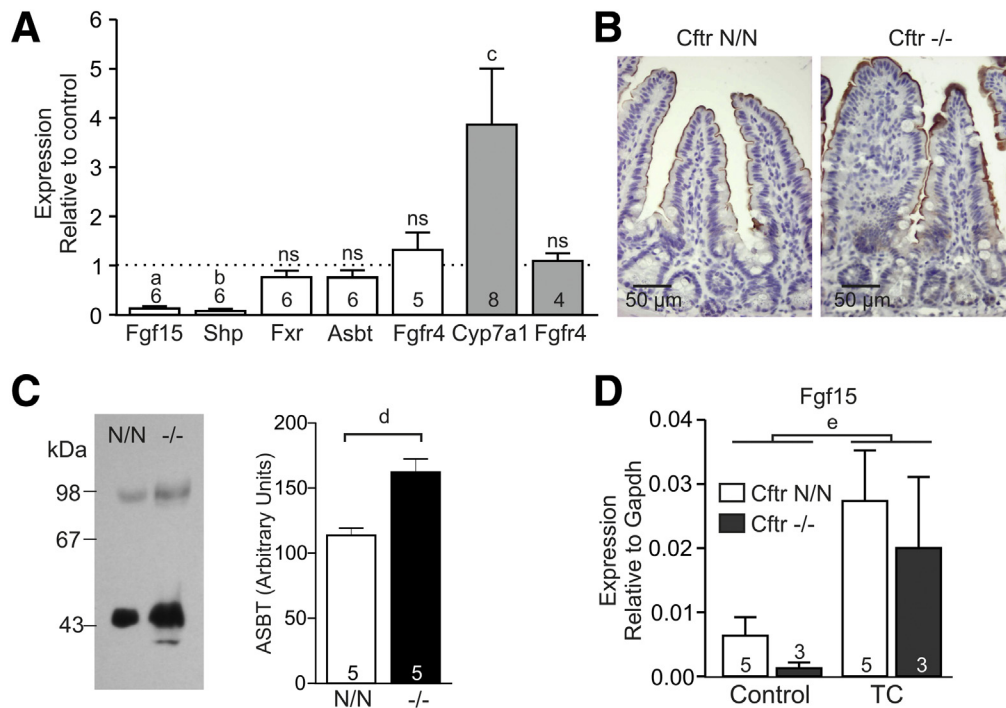


**Figure 1. FXR activity, ASBT localization, and taurocholic acid (TC)-dependent gene induction in the CF ileum.**

(A) Expression of genes involved in bile acid signaling in the ileum (*Fgf15*, *Shp*, *Fxr*, *Asbt*, *Fgfr4*) and liver (shaded bars; *Cyp7a1*, *Fgfr4*) of CF mice (*Cftr*<sup>-/-</sup>) and controls (*Cftr* N/N). Data represent expression in a CF animal relative to an age-/sex-matched littermate control (means  $\pm$  SE). The number of couples analyzed is indicated within/above each bar. a,  $P = .005$ ; b,  $P = 0.001$ ; c,  $P = .005$ ; ns,  $P > .05$  (paired ratio *t* test). (B) Immunohistochemical detection of ASBT in ileum of CF mice (*Cftr*<sup>-/-</sup>) and controls (*Cftr* N/N). ASBT was localized at the apical aspect of epithelial cells of the villi, but was absent from crypts. (C) ASBT was detected by Western analysis in brush-border membranes prepared from CF (-/-) and control (N/N) ileum. Both the monomeric (46 kilodaltons) and dimeric form were detected. Numerals to the left of the blot refer to the molecular mass (kilodaltons) of protein standards. ASBT abundance was quantified on the basis of the immune-reactive signal of both the monomer and dimer (*bar diagram*). Data shown are means  $\pm$  SE of 5 mice per genotype. d,  $P = .03$  (paired *t* test, 2-tailed). (D) Induction of gene expression by TC in ileal tissue sections of CF mice (*Cftr*<sup>-/-</sup>) and controls (*Cftr* N/N). Data shown are means  $\pm$  SE. The number of biological replicates is indicated within/above each bar. e, Two-way analysis of variance indicated that TC treatment significantly enhanced *Fgf15* expression ( $P = .006$ ), independent of genotype.

web 4C/FPO

We hypothesized that a shortage of activating ligands may have attenuated FXR signaling, possibly as a result of reduced ASBT-mediated BA uptake. Therefore, we assessed the expression and localization of ASBT. In the distal ileum, the messenger RNA level of *Asbt* (*Slc10a2*) was similar in CF mice and controls (Figure 1A). By immunohistochemistry, ASBT was localized at the apical plasma membrane of enterocytes in the villi, but absent from cells in the crypts of Lieberkuhn, and this pattern was unaffected by CFTR deficiency (Figure 1B). Consistent with this localization pattern, ASBT was detected in ileal brush-border membrane preparations, and appeared more abundant in preparations from CF mice than in controls (Figure 1C). When ileal tissue sheets of CF mice and controls were exposed to taurocholic acid, *Fgf15* was induced to a similar extent in both groups (Figure 1D). These findings argue against a primary defect in cellular BA uptake.

### CFTR Deficiency Affects the Composition, but Not the Size, of the Luminal BA Pool

Because, ex vivo, FXR could be fully activated by exogenous BAs, we hypothesized that, in vivo, FXR activation

may be curtailed by a low luminal BA level, as was suggested previously.<sup>18</sup> Therefore, we assessed the levels of the major BAs in the small intestinal lumen and in gastrointestinal tissues. This analysis showed that the BA content of the small intestinal lumen was similar in CF mice and controls (Figure 2A). The total amount of BA contained in the 4 compartments analyzed (representing most of the total pool) also was similar between genotypes. However, the composition of the luminal BA pool was changed by CFTR deficiency:  $\beta$ -muricholic acid ( $\beta$ -MCA) levels were markedly lower, whereas CA levels were higher than in control mice (Figure 2B). We previously observed that hepatic CA synthesis was enhanced in CF mice, leading to a similar shift in the biliary  $\beta$ -MCA/CA ratio.<sup>17</sup> Low ileal *Fgf15* expression, enhanced hepatic BA synthesis, and low biliary  $\beta$ -MCA/CA ratios have been linked to enhanced intraluminal conversion (deconjugation, dehydroxylation) of BAs upon gut microbiota modulation by probiotic bacterial strains.<sup>22</sup> However, arguing against enhanced intraluminal biotransformation, the level of the secondary BA deoxycholic acid in the small intestinal lumen was similar in CF mice and controls (Figure 2B). Therefore, although the luminal BA

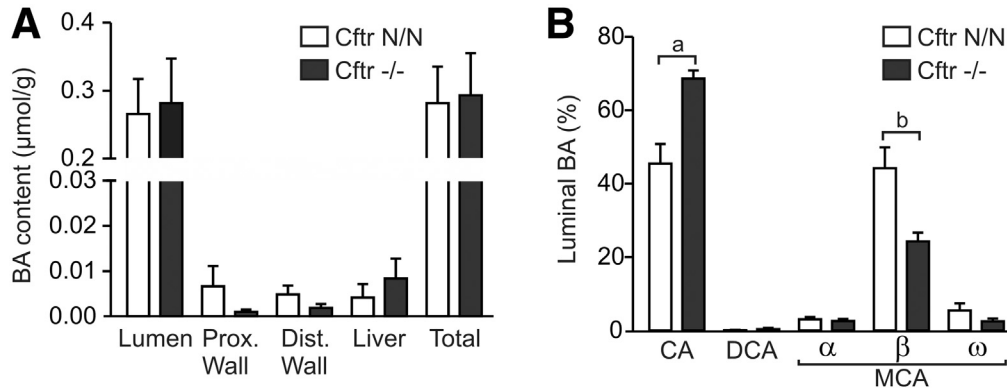


**Figure 2. Partitioning of BAs in gastrointestinal tissues and composition of the luminal BA pool.** (A) BA content, normalized to body mass, of the small intestinal lumen and gastrointestinal tissues in CF mice and controls. The total levels shown are a summation of the 4 separate compartments analyzed. (B) The relative contribution of the major BAs to the luminal pool. Data shown are means  $\pm$  SE of 5 *Cfr* N/N and 4 *Cfr* -/- mice. a,  $P = .02$ ; b,  $P = .008$  (t test, 2-tailed). DCA, deoxycholic acid; Dist, distal; Prox, proximal.

composition in CF mice is indicative of enhanced hepatic BA synthesis, in line with attenuated FXR/FGF15 signaling, it does not provide evidence for reduced intestinal BA delivery or enhanced BA biotransformation.

### CFTR Deficiency Affects the Host–Microbe Interaction

Phylum-specific primer sequences within the bacterial 16S ribosomal RNA gene were used to assess the microbial composition of the distal small intestine of CF and wild-type mice. This showed that the bacterial community in the distal small intestine consisted predominantly of *Bacteroidetes* (58%) and *Firmicutes* (28%) (Figure 3A). The relative abundance of other phyla was comparatively low. In CF mice, the relative abundance of *Bacteroidetes* (22%) was lower whereas that of *Firmicutes* (55%) was higher than in controls (Figure 3A). It has been shown that dysbiosis impacts intestinal architecture, leading to a lengthening of the gut.<sup>30</sup> Presently, we found that even though CF mice have a significantly lower body mass than wild types (Figure 3B), their small intestine was 6% (normalized to body mass: 28%) longer than that of controls (Figure 3C).

The ileal expression of  $\beta$ -1,4-galactosyltransferase I (*B4galt1*) and fuc  $\alpha$ 1-2 fucosyltransferase (*Fut2*), enzymes that catalyze glycosylation of secreted mucin proteins, was up-regulated in CF mice (Figure 3D). *Fut2* is known to be induced by bacterial colonization of the gut and was shown to enhance fucosylation of mucins in CF mice, whereas, interestingly, overexpression of *B4galt1* was shown to increase the *Firmicutes* to *Bacteroidetes* ratio in the mouse gut.<sup>31–34</sup> The expression of several inflammation markers, including acute-phase proteins (*Saa1*, *Saa3*), chemokines/cytokines (*Ccl8*, *Cxcl9*, the alarmin *Il33*), and antimicrobial peptides (*Ltf*), also was higher in CF mice than in controls (Figure 3D). Analysis of the ileal transcriptome indicated an up-regulation of genes involved in Toll-like receptor (TLR) signaling in CF mice, consistent with an altered host–microbe interaction (Figure 3E).

### Antibiotic Treatment Corrects FXR Signaling in CF Mice

In view of the tentative role of the gut microbiota in the regulation of FXR activity, we assessed the effect of antibiotic treatment on FXR signaling. Previously, it was shown that complete eradication of the microflora strongly reduced *Fgf15* expression because the gut microbiota appears to control the level of the FXR antagonist tauro- $\beta$ -MCA.<sup>20</sup> Therefore, a relatively mild antibiotic regimen was applied, which previously was shown not to eradicate the microflora fully, but to reduce small intestinal bacterial overgrowth in CF mice.<sup>28</sup> As a testament to its effectiveness, this treatment markedly reduced the expression of typical inflammation markers in CF mice (Figure 4A). Importantly, it also restored *Fgf15* and *Shp* expression in CF mice up to the level observed in control animals, in which antibiotic treatment did not induce *Fgf15* or *Shp* (Figure 4B). In fact, antibiotic treatment appeared to moderately reduce the expression of *Fgf15* in controls, suggesting that even this mild treatment leads to increased tauro- $\beta$ -MCA levels and repression of FXR activity. If present, this antagonistic action of tauro- $\beta$ -MCA is apparently offset by a dominant FXR stimulatory effect in CF mice. Concomitant with induction of *Fgf15*, hepatic expression of *Cyp7a1* was reduced in CF mice (Figure 4C). The hepatic expression of the FGF15 receptor, *Fgfr4*, was reduced moderately by antibiotic treatment in both genotypes (Figure 4C).

### Bacterial Lipopolysaccharide and Proinflammatory Cytokines Abrogate FXR-Dependent *Fgf15* Induction

In ileal organoids grown under microbe-free conditions, the synthetic FXR agonist GW4064 strongly induced *Fgf15*, and the level of expression attained was similar in CF and control organoids (Figure 5A). Lipopolysaccharide (LPS) did not notably affect GW4064-dependent expression of *Fgf15* or *Nr0b2* in organoids, but combined administration of interferon  $\gamma$ , tumor necrosis factor  $\alpha$ , and interleukin  $1\beta$

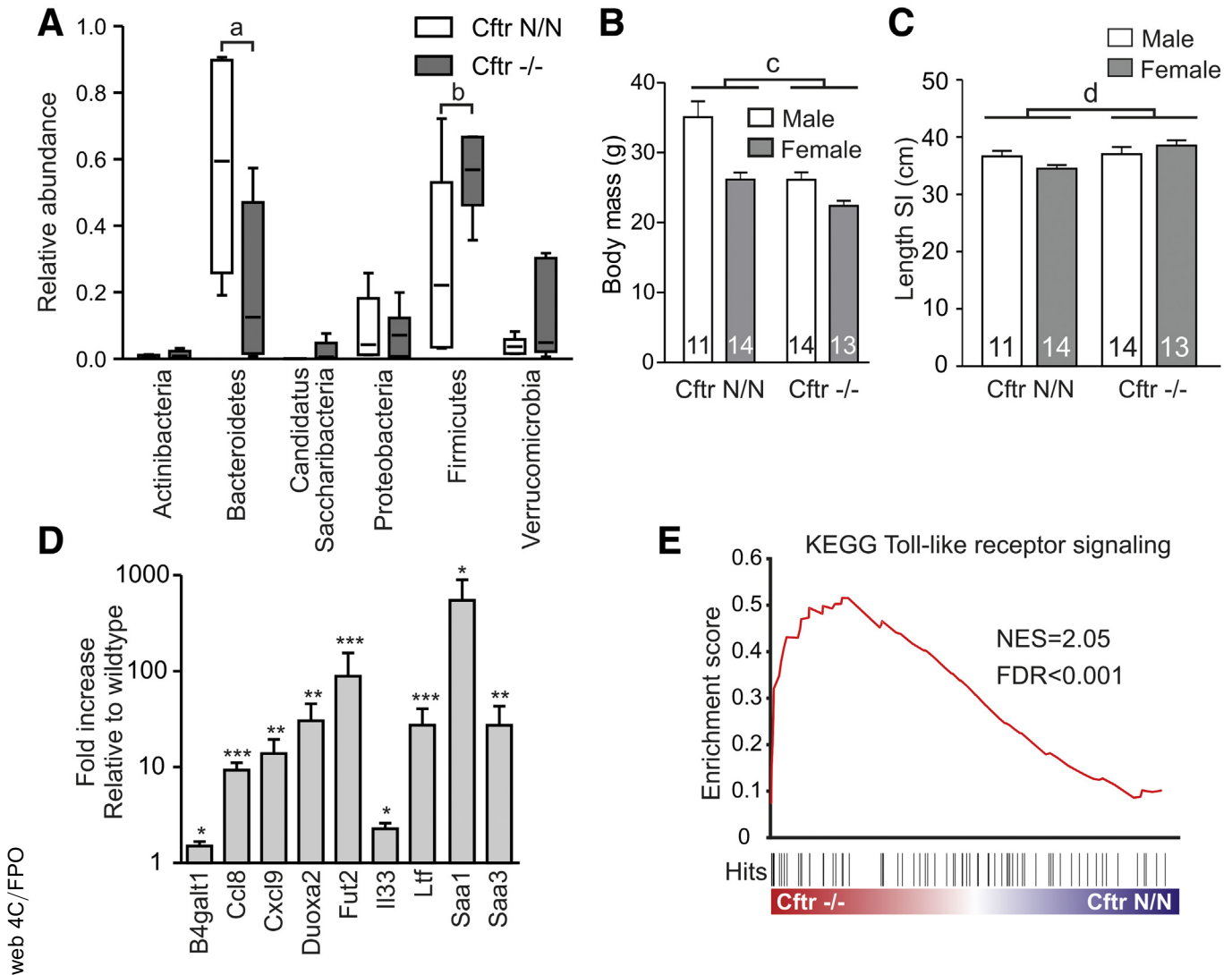


**Figure 3. CFTR deficiency affects the host-microbe interaction.** (A) The relative abundance of major bacterial phyla in the distal small intestine of CF mice and controls. *Box-and-whisker plot* showing means, range, and 5th–95th percentile of 6 animals per genotype. *a*,  $P = .048$ ; *b*,  $P = .047$  (*t* test, 2-tailed). (B) Body mass of male and female CF mice (*Cftr*<sup>-/-</sup>) and controls (*Cftr*<sup>N/N</sup>). Data shown are means  $\pm$  SE. The number of animals per group is indicated within each *bar*. *c*, Two-way analysis of variance indicated that CFTR loss had a statistically significant ( $P < .0001$ ) effect on body mass. (C) Length of the small intestine (SI) in male and female CF mice (*Cftr*<sup>-/-</sup>) and controls (*Cftr*<sup>N/N</sup>). Data shown are means  $\pm$  SE. The number of animals per group is indicated within each *bar*. *d*, Two-way analysis of variance indicated that CFTR loss had a statistically significant ( $P = .03$ ) effect on intestinal length, independent of sex. (D) Transcript levels of genes involved in the host-microbe interaction in ileum of CF mice, relative to sex-matched littermate controls. Data shown are means  $\pm$  SE of 6 couples. \* $P < .05$ , \*\* $P < .01$ , and \*\*\* $P < .001$  (paired ratio *t* test, 2-tailed). (E) Gene set enrichment analysis enrichment plot of the Kyoto Encyclopedia of Genes and Genomes (KEGG) Toll-like receptor signaling gene set.

lowered GW4064-dependent induction of *Nr0b2*, and also tended to repress induction of *Fgf15* (Figure 5B). In ileal tissue explants, LPS abrogated GW4064-dependent *Fgf15* expression, in line with previous data showing that proinflammatory cytokines suppress intestinal FXR activity (Figure 5C).<sup>35</sup>

### Impaired Intestinal FXR Signaling Reduces BA-Dependent Hepatic Cell Proliferation

FGF15-dependent hepatic cell proliferation was shown to promote liver regeneration after injury, and it was

proposed that this intestine-liver signaling axis also drives homeotrophic liver growth/repair.<sup>6,7,36</sup> It was shown that, through activation of this axis, dietary CA supplementation increases liver mass.<sup>36</sup>

To investigate whether impaired FXR/retinoid X receptor signaling in the CF intestine affects this intestine-liver signaling axis, we assessed the effect of dietary CA supplementation on liver mass, and intestinal and hepatic expression of FXR target genes. We found that CA supplementation strongly induced *Fgf15* in both genotypes, but that this effect was markedly more pronounced in control than in CF mice (Figure 6A). FGF15 protein was detectable

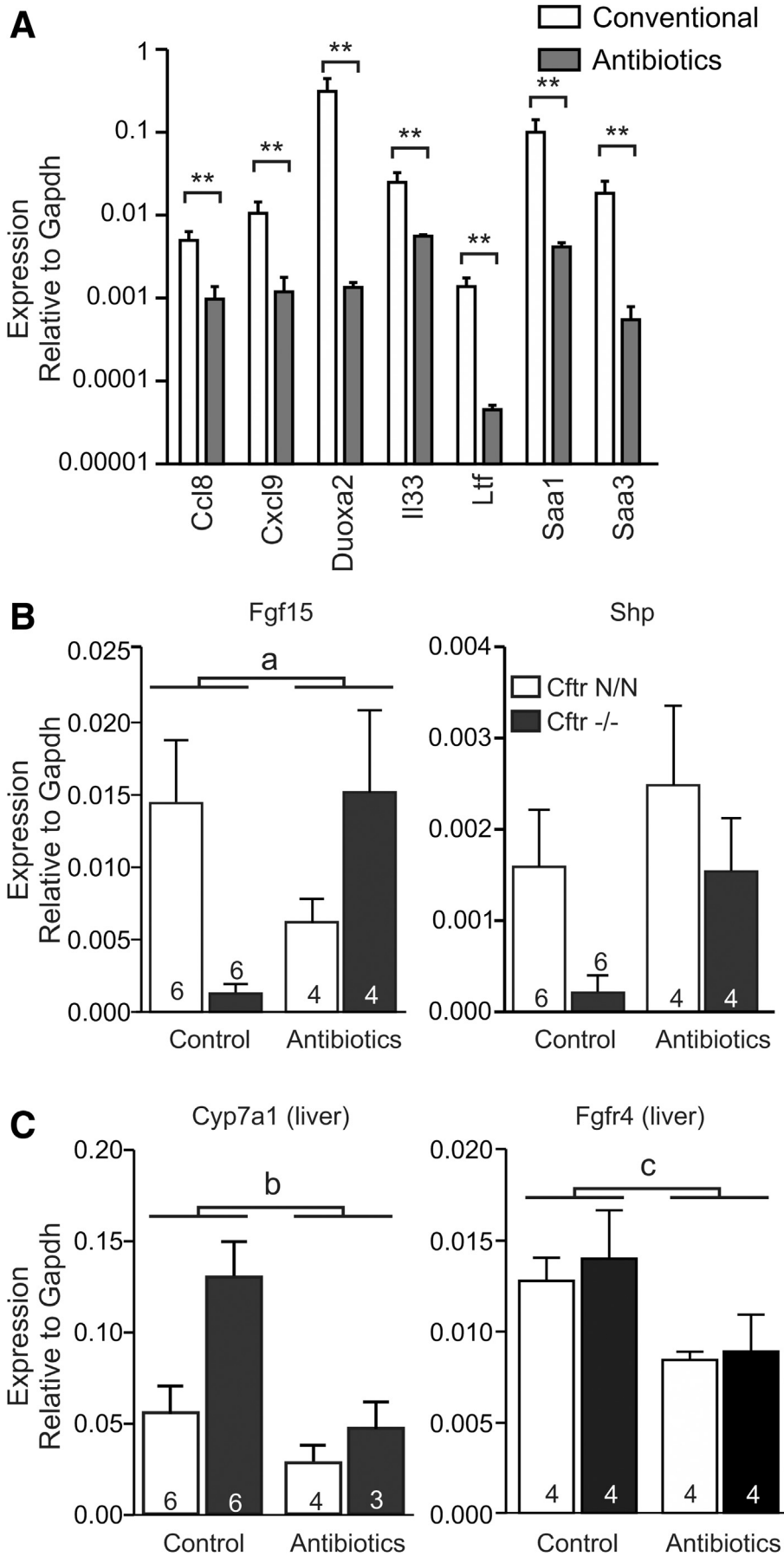


**Figure 4. The effect of antibiotic treatment on intestinal and hepatic gene expression.** (A) The effect of antibiotic treatment on the expression of typical inflammation markers in the ileum of CF mice. Data shown are means  $\pm$  SE of 6 (Conventional) or 4 (Antibiotics) animals per group.  $**P < .01$  (Mann-Whitney *U* test, 2-tailed). (B) The effect of antibiotic treatment on ileal *Fgf15* and *Shp* expression in CF mice (*Cfr*<sup>-/-</sup>) and littermate controls (*Cfr*<sup>N/N</sup>). Data shown are means  $\pm$  SE. The number of animals per group is indicated within/above each bar. a, Two-way analysis of variance indicated a statistically significant interaction between antibiotic treatment and *Cfr* genotype for *Fgf15* expression ( $P = .007$ ), implying that loss of CFTR affects the response to antibiotic treatment. (C) The effect of antibiotic treatment on hepatic *Cyp7a1* and *Fgfr4* expression (means  $\pm$  SE). The number of animals per group is indicated within/above each bar. (b) Two-way ANOVA indicated that antibiotic treatment reduced hepatic *Cyp7a1* ( $P = .02$ ) expression. (c) Two-way ANOVA indicated that antibiotic treatment reduced hepatic *Fgfr4* expression ( $P = .02$ ). Gapdh, glyceraldehyde-3-phosphate dehydrogenase.

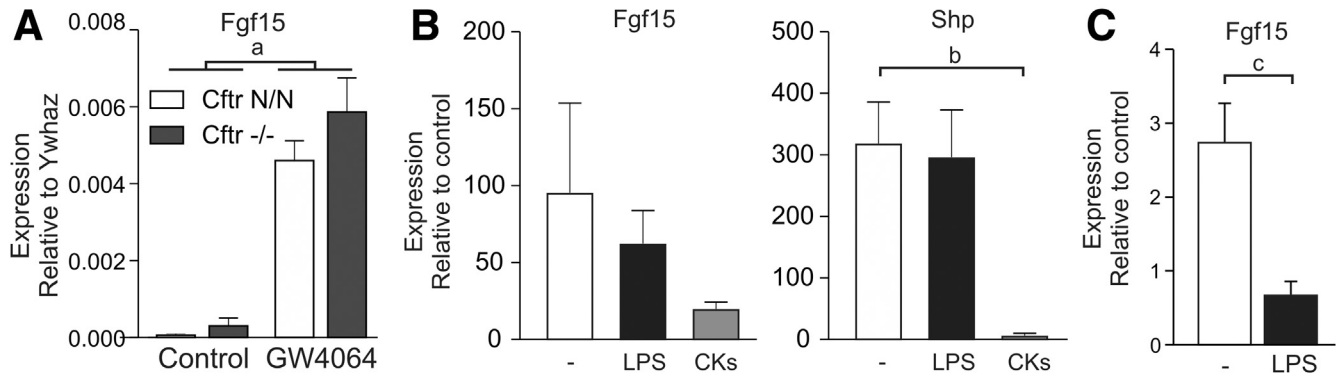


**Figure 5. Proinflammatory signaling inhibits FXR-dependent gene expression in mouse ileum.** (A) Induction of gene expression in ileal organoids derived from CF mice (*Cftr*<sup>-/-</sup>) and controls (*Cftr* N/N). Data shown are means  $\pm$  SE of 3 technical replicates per group. *a*, Two-way analysis of variance indicated that treatment with the FXR agonist GW4064 significantly enhanced *Fgf15* expression ( $P = .0002$ ), independent of genotype. (B) Induction of *Fgf15* and *Shp* expression by GW4064 in the presence or absence of LPS, or the cytokines (CKs) interferon  $\gamma$ , interleukin  $1\beta$ , and tumor necrosis factor  $\alpha$  (CKs), in ileal organoids. Data show the level of gene expression relative to the level of expression in the absence of GW4064. Data shown are means  $\pm$  SE of 4–6 technical replicates. *b*, One-way analysis of variance indicates that the combination of cytokines significantly reduced GW4064-dependent *Shp* expression ( $P = .02$ , Tukey multiple comparisons test). (C) Induction of *Fgf15* expression by GW4064 in the presence or absence of LPS in ileal tissue. Data show the level of gene expression relative to the level of expression in the absence of GW4064. Data shown are means  $\pm$  SE of 4 biological replicates. *c*, One-way analysis of variance indicates that LPS significantly reduced GW4064-dependent *Fgf15* expression ( $P = .007$ , Tukey multiple comparisons test).

by Western analysis only in ileal tissue lysates of CF and control mice fed CA, and levels were significantly lower in CF mice than in controls (Figure 6B). In mice fed a standard diet we were unable to detect FGF15 protein in either genotype, in line with the comparatively low transcript levels. In control mice, the strong stimulation of FGF15 production elicited by CA supplementation was associated with a marked increase in liver mass (Figure 6C). In contrast, in CF mice, this trophic response was lost completely. In accord with the low FGF15 production observed in CF mice, *Cyp7a1* expression was repressed much less effectively in CA-fed CF mice than in controls (Figure 6D). However, the regulation of genes that are controlled (predominantly) through hepatic FXR was not notably affected: CA supplementation repressed *Cyp8b1* expression and induced hepatic *Shp* to a similar extent in CF mice and controls (Figure 6D).<sup>2,5,37</sup>

## Discussion

This study shows that signaling through the BA-activated nuclear receptor FXR is impaired markedly in the distal small intestine of CF mice. Impaired intestinal FXR signaling compromised BA-dependent regulation of hepatic cell proliferation and BA synthesis. This defect was associated with dysbiosis and an up-regulation of genes involved in host–microbe interactions and innate immunity. Antibiotic treatment reduced the expression of inflammation markers and restored FXR activity in the CF ileum. FXR-dependent gene induction was not affected in CF organoids (grown under sterile conditions), but treatment with LPS or proinflammatory cytokines provoked a CF-like repression of FXR signaling in non-CF ileal tissue and organoids, respectively. These data suggest that a

CF-related inflammatory response represses signaling through FXR.

We observed strong repression of *Fgf15* and *Nr0b2*, 2 key targets of the BA-activated nuclear receptor FXR, in ileum of CF mice. Indeed, based on our transcriptome data, both of these FXR targets rank among the most strongly down-regulated genes in the CF intestine.<sup>38</sup> In line with a role of the gut microbiota in the down-regulation of FXR signaling, we observed a dysbiosis in CF mice and found that containment of bacterial growth (by antibiotic treatment) enhanced FXR signaling specifically in CF mice. Loss of CFTR-dependent chloride and bicarbonate secretion in the gut leads to luminal dehydration and acidification, which, in turn, leads to aberrant mucus production.<sup>39</sup> Mucus plugging, in conjunction with maldigestion and malabsorption, and a protracted intestinal transit, is thought to promote microbial colonization of the small intestine.<sup>40</sup> In our CF mice, dysbiosis was chiefly characterized by an increase in the *Firmicutes* to *Bacteroidetes* ratio, as has been observed similarly in murine models of colitis.<sup>41,42</sup> It was associated with an up-regulation of inflammation markers and gene set enrichment analysis indicated TLR activation. The observed up-regulation of the TLR-regulated *Fut2*, an enzyme that catalyzes fucosylation of secreted mucin proteins, also points toward an altered host–microbe interaction.<sup>31,34</sup> Because the glycosyl moieties of mucins are metabolized by bacteria, the activity of transferases such as *Fut2* and *B4galt1* may have a marked impact on the gut microbiota. For instance, a modest overexpression of *B4galt1*, as observed similarly in our CF mice, was shown to be sufficient to significantly increase the *Firmicutes* to *Bacteroidetes* ratio in the mouse gut, whereas deficiency of another glycosyltransferase, *C1galt1*, was shown to shift this ratio in the opposite direction.<sup>30,33</sup> Furthermore, aberrant mucin glycosylation and attendant changes in the gut

microbiota were shown previously to promote gut elongation, suggesting that the intestinal lengthening observed in CF mice may have similar causes.<sup>30,43</sup>

Both hepatic and intestinal FXR signaling were shown previously to be strongly repressed by bacterial endotoxins and proinflammatory cytokines.<sup>23–25,35</sup> We found that LPS abrogated FXR-dependent *Fgf15* induction in non-CF ileum, mimicking the strong repression of FXR activity observed in vivo in the CF intestine. Conversely, FXR activity was restored in CF tissue, ex vivo, and in CF organoids, indicating that the repression is readily reversible. Proinflammatory cytokines, but not LPS, repressed FXR-dependent gene induction in organoids, suggesting that the action of LPS in tissue depends on cytokine release from nonepithelial cell types, and/or that expression of genes required for LPS signaling, such as TLR4, is lost in epithelial cell cultures. These data indicate that a bacterial endotoxin-induced inflammatory response can impair FXR function in the gut, and strongly suggest that local inflammation of the gut wall represses FXR activity in the CF ileum. In this context, it is of interest that CF mice, including the strain presented here, also show impaired intestinal peroxisome proliferator-activated receptor- $\gamma$  signaling because inactivation of peroxisome proliferator-activated receptor- $\gamma$  was shown to promote colonization of the gut by (LPS-producing) gram-negative facultative anaerobes.<sup>38,44–46</sup>

It has been reported that intraluminal bacterial modification (deconjugation, dehydroxylation) of BAs may reduce their uptake via ASBT and, consequently, lower FXR activity.<sup>22</sup> However, the intraluminal levels of the secondary BA deoxycholic acid were similar in CF mice and controls, which argues against enhanced microbial metabolism of BAs. Moreover, although we and others previously have shown that fecal BA excretion is approximately 2-fold higher in CF mice than in controls, this amounts to only a modest reduction in the overall efficacy of the absorptive process because normally only 3%–5% of the dose entering the intestine through biliary secretion is lost.<sup>15,16,47</sup> It follows that the efficacy of the absorptive process is decreased from  $\geq 95\%$  in controls to approximately 90% in CF mice, and it is difficult to envisage how such a modest reduction in BA absorption could lead to the strong repression of FXR target genes observed. Similarly, the notion that intraluminal bioconversion limits FXR activity is difficult to reconcile with the observation that dietary CA supplementation did not fully restore FXR activity because the dose used in these experiments results in luminal CA levels well in excess of those occurring naturally and is predicted to saturate carrier-mediated absorption.<sup>48</sup> To exclude a defect in the latter process, we ascertained that the apical localization of this carrier, ASBT, was not affected. In fact, ASBT levels were higher (approximately 1.4-fold) in brush-border membrane preparations of CF mice than of controls. Conceivably, this increase is linked to decreased *Fgf15* expression because it has been shown that FGF15/hepatic receptor of FGF15 (FGFR4) signaling reduces ASBT protein abundance in mouse ileum.<sup>49</sup> Collectively, these data suggest that intestinal FXR activity is limited primarily by a defect located downstream of cellular BA uptake.

In mice, complete FGF15 deficiency was shown to markedly enhance hepatic *Cyp7a1* expression and the fecal excretion of BAs.<sup>5</sup> Our current findings indicate that low FGF15 production and impaired feedback regulation of BA synthesis similarly may contribute to the fecal BA wasting observed in CF mice.<sup>15,16</sup> Congruent with this concept, we have observed previously that the antibiotics used at present reduce the fecal excretion of cholic acid in CF mice.<sup>50</sup> This model also may explain why some have observed that biliary BA secretion is enhanced in CF mice.<sup>16</sup> It also accounts for the fact that the presentation of fecal BA wasting in patients is quite variable because any factor that affects host–microbe interactions and gut immunity may modulate BA handling. The same probably holds true for CF mouse models, and this may explain why effects on fecal excretion and biliary secretion of BAs may be subtle and escape detection.<sup>17,18,51</sup> One key confounding factor is the diet: CF mice almost invariably are reared on liquid elemental formulations or oral laxatives (to prevent intestinal obstruction), both of which markedly affect the bacterial load in the gut.<sup>52,53</sup> Indeed, recently, we showed that application of an oral laxative with a high polyethylene glycol/low electrolyte composition (ie, different from the formulation used in our present study), reduced fecal BA excretion in CF (*Cfr*<sup>tm1Unc</sup>) mice.<sup>54</sup>

We observed that the hepatic trophic response, induced by BA-dependent induction of intestinal *Fgf15*, is strongly suppressed in CF mice. Because this signaling axis was proposed to play a role in the homeostatic control of liver regeneration after injury, we surmise that an intestinal FXR signaling defect also may be of consequence for the pathophysiology of CFLD.<sup>6,7</sup> Impaired intestinal FXR signaling also may enhance exposure of the liver to endotoxins because it was shown that FXR deficiency, in conjunction with dysbiosis, compromises epithelial barrier function.<sup>55</sup> Congruent with this scenario, it was shown that a chemically induced colitis exacerbates liver disease in CF mice, and a pathogenic role of gut-derived bacterial products was indicated.<sup>12</sup> Decreased intestinal FGF19 production and an attendant increase in BA synthesis may contribute further to the progression of the cholangiopathy.<sup>6,8,9</sup> Indeed, although focal biliary cirrhosis is thought to result primarily from the loss of local CFTR activity, it also is apparent that some gastrointestinal manifestations of CF that are likely to impact the gut microbiota, such as pancreatic insufficiency and a history of meconium ileus, seem to predispose to the development of CFLD.<sup>11,56,57</sup> Collectively, these data imply that intestinal inflammation and FXR dysfunction may contribute to the pathogenesis of biliary cirrhosis, suggesting that therapeutic interventions aimed at restoring FXR signaling may slow its progression.

## Methods

### Animal Procedures and Tissue Collection

CF mice (*Cfr*<sup>tm1Cam</sup>; congenic FVB/n) and littermate controls were maintained in individually ventilated cages in an environmentally controlled facility at the Erasmus Medical Center. Animals were reared on a low-fiber diet (C1013; Altromin, Lage, Germany) and a polyethylene



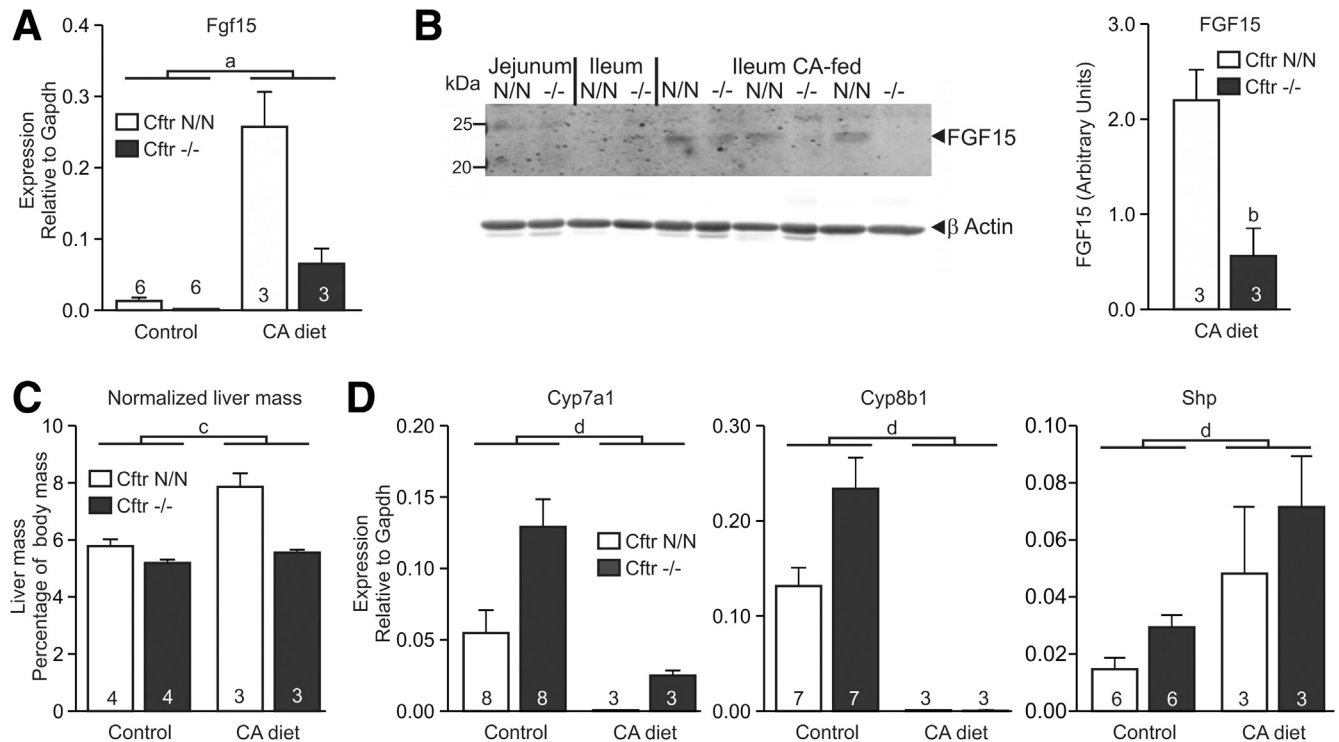


**Figure 6. The effect of dietary BA supplementation on FXR signaling.** CF mice (*Cfr*<sup>-/-</sup>) and controls (*Cfr*<sup>N/N</sup>) were fed a CA-enriched or a conventional diet. (A) Induction of intestinal *Fgf15* by CA. Data shown are means  $\pm$  SE. The number of animals per group is indicated within/above each bar. Control data as shown in Figure 4B. <sup>a</sup> Two-way analysis of variance indicated a significant interaction between CA intake and *Cfr* genotype for the effect on *Fgf15* expression ( $P = .0001$ ), implying that loss of CFTR affects the response to dietary CA supplementation. (B) FGF15 protein was below detection levels in jejunal and ileal tissue of mice fed a control diet. CA feeding increased FGF15 levels in both CF mice and controls, but this effect was more pronounced in controls. Numerals to the left of the blot refer to the molecular mass (kilodaltons) of protein standards. The bar diagram shows the intensity of the fluorescent signal of the FGF15 band relative to the  $\beta$ -actin signal of the same sample. Data shown are means  $\pm$  SE of 3 animals per genotype. <sup>b</sup>  $P = .02$  (*t* test, 2-tailed) (C) Effect of CA supplementation on liver mass. Data shown are means  $\pm$  SE. The number of animals per group is indicated within/above each bar. <sup>c</sup> Two-way analysis of variance indicated a statistically significant interaction between CA feeding and *Cfr* genotype for the effect on liver mass ( $P = .004$ ), implying that loss of CFTR affects the response to dietary CA supplementation. (D) Effect of dietary BA supplementation on hepatic gene expression. Data shown are means  $\pm$  SE. The number of animals per group is indicated within/above each bar. <sup>d</sup> Two-way analysis of variance indicated that CA feeding suppressed hepatic *Cyp7a1* ( $P = .001$ ) and *Cyp8b1* ( $P = .0001$ ) expression, but enhanced expression of *Shp* ( $P = .003$ ). Gapdh, glyceraldehyde-3-phosphate dehydrogenase.

glycol/electrolyte dinking solution to prevent intestinal obstruction in early life (22.8 g/L polyethylene glycol 4000: 40 mmol/L  $\text{Na}_2\text{SO}_4$ , 75 mmol/L  $\text{NaHCO}_3$ , 10 mmol/L NaCl, and 10 mmol/L KCl).<sup>58</sup> In some instances, before further experimentation, animals were administered either a diet supplemented with CA (0.5%), or drinking water supplemented with ciprofloxacin (0.3 g/L) and metronidazole (0.5 g/L) for 15 days.<sup>28</sup> Intake of food and water was monitored during this period and shown to be comparable between genotypes (not shown).

Before tissue collection, animals (age, 13–22 wk) were kept on normal drinking water (or, when applicable, drinking water supplemented with antibiotics) for >4 days, which is well tolerated by adult CF mice. Animals were anesthetized (120 mg/kg ketamine, 20 mg/kg xylazine; intraperitoneally), and the intestinal tract and liver were collected, and flushed or rinsed, respectively, with ice-cold saline. Sampling from a CF animal and a sex-matched littermate control was performed within a time window of

20 minutes, and between 12:00 and 14:00 hours, to control for diurnal variations in gene expression. Experiments were approved by the Independent Committee on Ethical Use of Experimental Animals (Rotterdam, The Netherlands), according to national guidelines (120-0402/0501/0503/0902; 141-1204/1208/1210).

### Intestinal and Hepatic Gene Expression

For gene expression studies, 2 ileal sections (length, 3–5 mm) were collected, at 0.5–1.5 and 5–6 cm proximal to the ileocecal valve. Liver tissue was sampled from the right lobe. Tissue homogenization, RNA extraction, and quantitative reverse-transcriptase polymerase chain reaction (primer sequences shown in Table 1) was performed as described elsewhere.<sup>59</sup> Median values of assays performed in triplicate were used to determine gene expression levels, relative to *Gapdh*. To correct for regional differences in gene expression in the distal small intestine, mean values of the

relative expression levels at the 2 sampling locations are presented.

### Gut Microbiota Analysis

The content of the distal small intestine (one third of its total length) was collected by flushing with 10 mL of ice-cold phosphate-buffered saline, and samples were stored at -20°C until further analysis. After thawing, the intestinal contents were collected by centrifugation (4000 × g; 30 min), and microbial DNA was extracted using an RTP Bacteria DNA Mini Kit, according to the manufacturer's instructions (Strattec Molecular, Berlin, Germany). Real-time polymerase chain reaction was performed on the isolated DNA using phylum-specific primer sequences within the 16S ribosomal RNA gene to assess the composition of the ileal microbiota, as described in detail elsewhere.<sup>60</sup>

### Organoid Culture

Organoid cultures were initiated from isolated intestinal crypts, harvested from the distal small intestine (up to 8-cm proximal to the ileocecal valve), as described in detail elsewhere.<sup>61</sup> Briefly, organoids were cultured, embedded in Matrigel (Corning Life Sciences, Amsterdam, The Netherlands), in medium containing epidermal growth factor, noggin, R-spondin 1, and WNT3a. Cell differentiation was prompted by culturing in the absence of WNT3a, in medium containing the WNT secretion inhibitor IWP-2 (10 μmol/L; Tocris, Abingdon, United Kingdom).

### Ex Vivo FXR-Dependent Induction of Intestinal Gene Expression

For assessing BA-dependent induction of gene expression, 2 contiguous sections of the small intestine were

collected 3–5 cm proximal to the ileocecal valve. Mucosal tissue sheets were mounted in Ussing chambers and bathed in modified Meyler solution, gassed with 95% O<sub>2</sub>–5% CO<sub>2</sub>, at 37°C, as described previously.<sup>62</sup> After a 40-minute equilibration period, the solution bathing the luminal side of 1 tissue sheet was supplemented with taurocholic acid (0.25 mmol/L), while the other section served as vehicle (water) control. After 1 hour, tissue was collected and processed for RNA extraction (see Intestinal and Hepatic Gene Expression). For assessing the effect of bacterial LPS on FXR-dependent gene induction, ileal tissue sections were incubated for 18 hours with the FXR agonist GW4064 (1 μmol/L; Selleck Chemicals, Munich, Germany), in the presence or absence of LPS (*Salmonella enterica*; 10 μg/mL), in Dulbecco's modified Eagle medium, supplemented with fetal calf serum (10%), penicillin (50 U/mL), and streptomycin (0.005%), at 37°C in 5% CO<sub>2</sub>.

Organoids, cultured for 5 days in differentiation medium (see Organoid Culture), were cultured for 20 hours in the presence or absence of LPS (10 μg/mL) or a combination of cytokines (200 ng/mL murine interferon γ, 50 ng/mL tumor necrosis factor α, 10 ng/mL IL1β; Peprotech, Rocky Hill, NJ). FXR-dependent gene induction was prompted by the addition of GW4064 (1 μmol/L, 4 h). Organoids were harvested in ice-cold phosphate-buffered saline, collected by centrifugation (300 X g, 5 min), and processed for RNA extraction.<sup>59</sup> Gene expression was assessed as outlined above for tissue, using *Ywhaz* expression as a reference.

### Detection of ASBT and FGF15 by Western Blot Analysis

For ASBT detection, brush-border membrane fractions were prepared from the distal 8 cm of the small intestine, as

**Table 1.** Primer Sequences

Gene	Accession	Forward primer	Reverse primer
<i>B4galt1</i>	NM_022305	GTTCCGGTTTACCTGCCAT	TTCTCCTCCCCAACCCCAAT
<i>Ccl8</i>	NM_021443	GGGTGCTGAAAAGCTACGAG	CATACCCTGCTTGGTCTGGAA
<i>Cxcl9</i>	NM_008599	CGAGGCACGATCCACTACAA	AGGCAGGTTTGATCTCCGTT
<i>Cyp7a1</i>	NM_007824	ACTCTCTGAAGCCATGATGCAA	AGCGTTAGATATCCGGCTTCAA
<i>Cyp8b1</i>	NM_010012	TTGCAAATGCTGCCTCAACC	TAACAGTCGCACACATGGCT
<i>Duoxa2</i>	NM_025777	CCACCAATATCACCTGGCCG	GACACCGAAGAGCGTGAAGG
<i>Fgf15</i>	NM_008003	GTCCCTATGTCTCCAAGTCTCC	TTCTCCTGAAGGTACAGTCTCC
<i>Fgfr4</i>	NM_008011	AAGGTGGTCAGTGGGAAGTCTG	CATGCAGTATCTGGAGTCTCGG
<i>Fut2</i>	NM_001271993	AGTCTTCGTGGTTACAAGCAAC	TGGCTGGTGGCCCTCAATA
<i>Gapdh</i>	NM_001289726	TTCCAGTATGACTCCACTCACGG	TGAAGACACCAGTAGACTCCACGAC
<i>Il33</i>	NM_001164724	TCCTGCCTCCCTGAGTACATA	ATCCACACCGTCGCCTGATT
<i>Ltf</i>	NM_008522	CCGGTGCCCAAAGGATAGA	CTCAGACACCTCAAGGCTCC
<i>Nr0b2</i>	NM_011850	CGAATCCTCCTCATGGCCTC	TCCCATGATAGGGCGGAAGA
<i>Nr1h4</i>	NM_001163700	CATCAAGGACAGAGAGGCGG	TCAGCGTGGTGGTGGTTGAA
<i>Saa1</i>	NM_009117	GTCTGGGCTTCTTCTACCTA	CCTCTCCTCCTCAAGCAGTTA
<i>Saa3</i>	NM_011315	GTTACACGGACATGGAGCAGAGGA	GCAGGCCAGCAGTCCGGAAGTG
<i>Slc10a2</i>	NM_011388	GGAAGTGGCTCCAATATCCTG	GTTCCCGAGTCAACCCACAT
<i>Ywhaz</i>	NM_011740	AATGAGCTGGTGCAGAAGGC	GAGCAGGCAGAGCGATATGA

described in detail elsewhere.<sup>63</sup> For FGF15 detection, ileal tissue was excised 2–5 cm proximal to the ileocecal valve, and epithelial cells were gently scraped off the underlying connective tissue layers, using a glass coverslip. Cells were lysed by brief sonication (three 15-s bursts) in ice-cooled NaCl (150 mmol/L), Tris/HCl pH 7.6 (25 mmol/L), Triton (Sigma Aldrich, St. Louis, MO) X-100 (1%), sodium deoxycholate (1%), sodium dodecyl sulfate (0.1%), NaF (5 mmol/L), and Na<sub>3</sub>VO<sub>4</sub> (3 mmol/L), supplemented with a protease inhibitor cocktail. Brush-border and whole-cell preparations were subjected to sodium dodecyl sulfate–polyacrylamide gel electrophoresis, and proteins were transferred to a nitrocellulose membrane. ASBT was detected using a polyclonal antibody directed against hamster ASBT.<sup>64</sup> FGF15 was detected using a polyclonal antibody directed against an epitope of mouse origin (SC27177; Santa Cruz, Dallas, TX). A fluorescent dye–labeled secondary antibody and the Odyssey infrared imaging system (Application software 3; Licor Biosciences, Bad-Homburg, Germany) were used for quantification. Detection of  $\beta$ -actin served as loading control (SC47778; Santa Cruz).

### Immunohistochemistry

Paraformaldehyde-fixed, paraffin-embedded tissue sections (5  $\mu$ m) of the distal small intestine (excised 2–4 cm proximal to the ileocecal valve) were probed with a polyclonal antiserum directed against hamster ASBT (1:100; see above), followed by an anti-rabbit IgG horseradish-peroxidase–conjugated secondary antibody. Immune complexes were visualized by incubation with 3,3'-diaminobenzidine tetrahydrochloride, in sections counterstained with hematoxylin [Zeiss [Oberkochen, Germany] Axioskop 20 microscope and a Nikon [Amsterdam, Netherlands] DS-U1 camera].

### Analysis of BA in Luminal Eluates and Gastrointestinal Tissues

Tissue was collected from anesthetized animals, as outlined above. To collect its contents, the intestinal lumen was rinsed with 10 mL ice-cold phosphate-buffered saline. The intestine subsequently was divided into a proximal section (two thirds of the entire length) and a distal section. Tissue samples and eluates were weighed and the former were homogenized in ice-cold phosphate-buffered saline. After samples were saponified in NaOH (1 mol/L, in methanol), BAs were extracted on Sep-Pak C18 cartridges (Mallinckrodt Baker, Staines-Upon-Thames, United Kingdom). BAs were analyzed as unconjugated methyl ester-trimethylsilyl ether derivatives by capillary gas chromatography.<sup>65</sup>

### Data Analysis

The statistical significance of differences between mean levels of gene expression, ASBT and FGF15 abundance, tissue BA levels, and microbial composition in CF and controls were analyzed by Student *t* test (2-sided). The effect of GW4064, cytokines, and LPS on gene expression was analyzed by 1-way analysis of variance. The effect of BA and antibiotic treatment on gene expression in CF mice and

controls, and the effect of GW4064 on gene expression in CF and control organoids, was analyzed by 2-way analysis of variance. The Mann–Whitney *U* test was used to assess differences between data sets that were not normally distributed. Statistical analyses were performed using GraphPad Prism 5 (GraphPad Software, San Diego, CA).

For gene set enrichment analysis (Broad Institute, Cambridge, MA), transcriptome data from 3 sex-matched (2 females/1 male) littermate couples were used (NCBI-GEO repository GSE92991).<sup>38</sup> Gene set enrichment analysis was used to compare the expression profile observed in the data set with a priori–defined gene sets that represent well-defined biological processes (Kyoto Encyclopedia of Genes and Genomes curated gene sets; Molecular Signatures database 6.1; Broad Institute).<sup>66</sup> The degree to which genes in the predefined set are over-represented at the extremes of the ranked list of transcripts in the sample is reflected by the enrichment score.<sup>67</sup> To adjust for differences in gene set size, enrichment scores were normalized and statistically assessed using a correction for multiple hypotheses testing. The reported false-discovery rate is the estimated probability that the observed normalized enrichment score constitutes a false-positive result.

### References

- Hofmann AF. Biliary secretion and excretion in health and disease: current concepts. *Ann Hepatol* 2007;6:15–27.
- Kim I, Ahn SH, Inagaki T, Choi M, Ito S, Guo GL, Kliewer SA, Gonzalez FJ. Differential regulation of bile acid homeostasis by the farnesoid X receptor in liver and intestine. *J Lipid Res* 2007;48:2664–2672.
- Jung D, Inagaki T, Gerard RD, Dawson PA, Kliewer SA, Mangelsdorf DJ, Moschetta A. FXR agonists and FGF15 reduce fecal bile acid excretion in a mouse model of bile acid malabsorption. *J Lipid Res* 2007;48:2693–2700.
- Song KH, Li T, Owsley E, Strom S, Chiang JY. Bile acids activate fibroblast growth factor 19 signaling in human hepatocytes to inhibit cholesterol 7 $\alpha$ -hydroxylase gene expression. *Hepatology* 2009;49:297–305.
- Inagaki T, Choi M, Moschetta A, Peng L, Cummins CL, McDonald JG, Luo G, Jones SA, Goodwin B, Richardson JA, Gerard RD, Repa JJ, Mangelsdorf DJ, Kliewer SA. Fibroblast growth factor 15 functions as an enterohepatic signal to regulate bile acid homeostasis. *Cell Metab* 2005;2:217–225.
- Uriarte I, Fernandez-Barrena MG, Monte MJ, Latasa MU, Chang HC, Carotti S, Vespasiani-Gentilucci U, Morini S, Vicente E, Concepcion AR, Medina JF, Marin JJ, Berasain C, Prieto J, Avila MA. Identification of fibroblast growth factor 15 as a novel mediator of liver regeneration and its application in the prevention of post-resection liver failure in mice. *Gut* 2013;62:899–910.
- Zhang L, Wang YD, Chen WD, Wang X, Lou G, Liu N, Lin M, Forman BM, Huang W. Promotion of liver regeneration/repair by farnesoid X receptor in both liver and intestine in mice. *Hepatology* 2012;56:2336–2343.

8. Modica S, Petruzzelli M, Bellafante E, Murzilli S, Salvatore L, Celli N, Di Tullio G, Palasciano G, Moustafa T, Halilbasic E, Trauner M, Moschetta A. Selective activation of nuclear bile acid receptor FXR in the intestine protects mice against cholestasis. *Gastroenterology* 2012;142:355–365.
9. Zhou M, Learned RM, Rossi SJ, DePaoli AM, Tian H, Ling L. Engineered fibroblast growth factor 19 reduces liver injury and resolves sclerosing cholangitis in Mdr2-deficient mice. *Hepatology* 2016;63:914–929.
10. Staufer K, Halilbasic E, Trauner M, Kazemi-Shirazi L. Cystic fibrosis related liver disease: another black box in hepatology. *Int J Mol Sci* 2014;15:13529–13549.
11. Lamireau T, Monnereau S, Martin S, Marcotte JE, Winnock M, Alvarez F. Epidemiology of liver disease in cystic fibrosis: a longitudinal study. *J Hepatol* 2004;41:920–925.
12. Fiorotto R, Scirpo R, Trauner M, Fabris L, Hoque R, Spirlì C, Strazzabosco M. Loss of CFTR affects biliary epithelium innate immunity and causes TLR4-NF-kappaB-mediated inflammatory response in mice. *Gastroenterology* 2011;141:1498–1508.
13. Strandvik B, Einarsson K, Lindblad A, Angelin B. Bile acid kinetics and biliary lipid composition in cystic fibrosis. *J Hepatol* 1996;25:43–48.
14. Van de Peppel IP, Doktorova M, Berkers G, De Jonge HR, Houwen RHJ, Verkade HJ, Jonker JW, Bodewes FAJA. Ivacaftor restores FGF19 regulated bile acid homeostasis in cystic fibrosis patients with an S1251N or a G551D gating mutation. *J Cyst Fibros* 2019;18:286–293.
15. Bijvelds MJC, Bronsveld I, Havinga R, Sinaasappel M, De Jonge HR, Verkade HJ. Fat absorption in cystic fibrosis mice is impeded by defective lipolysis and post-lipolytic events. *Am J Physiol* 2005;288:G646–G653.
16. Freudenberg F, Broderick AL, Yu BB, Leonard MR, Glickman JN, Carey MC. Pathophysiological basis of liver disease in cystic fibrosis employing a DF508 mouse model. *Am J Physiol* 2008;294:G1411–G1420.
17. Bodewes FA, Wouthuyzen-Bakker M, Bijvelds MJC, Havinga R, De Jonge HR, Verkade HJ. Ursodeoxycholate modulates bile flow and bile salt pool independently from the cystic fibrosis transmembrane regulator (Cftr) in mice. *Am J Physiol* 2012;302:G1035–G1042.
18. Debray D, Rainteau D, Barbu V, Rouahi M, El Mourabit H, Lerondel S, Rey C, Humbert L, Wendum D, Cottart CH, Dawson P, Chignard N, Housset C. Defects in gallbladder emptying and bile acid homeostasis in mice with cystic fibrosis transmembrane conductance regulator deficiencies. *Gastroenterology* 2012;142:1581–1591.
19. Bodewes FA, Bijvelds MJC, De Vries W, Baller JF, Gouw AS, De Jonge HR, Verkade HJ. Cholic acid induces a Cftr dependent biliary secretion and liver growth response in mice. *PLoS One* 2015;10:e0117599.
20. Sayin SI, Wahlstrom A, Felin J, Jantti S, Marschall HU, Bamberg K, Angelin B, Hyotylainen T, Oresic M, Backhed F. Gut microbiota regulates bile acid metabolism by reducing the levels of tauro-beta-muricholic acid, a naturally occurring FXR antagonist. *Cell Metab* 2013;17:225–235.
21. Out C, Patankar JV, Doktorova M, Boesjes M, Bos T, De Boer S, Havinga R, Wolters H, Boverhof R, Van Dijk TH, Smoczek A, Bleich A, Sachdev V, Kratky D, Kuipers F, Verkade HJ, Groen AK. Gut microbiota inhibit Asbt-dependent intestinal bile acid reabsorption via Gata4. *J Hepatol* 2015;63:697–704.
22. Degirolamo C, Rainaldi S, Bovenga F, Murzilli S, Moschetta A. Microbiota modification with probiotics induces hepatic bile acid synthesis via downregulation of the Fxr-Fgf15 axis in mice. *Cell Rep* 2014;7:12–18.
23. Kim MS, Shigenaga J, Moser A, Feingold K, Grunfeld C. Repression of farnesoid X receptor during the acute phase response. *J Biol Chem* 2003;278:8988–8995.
24. Beigneux AP, Moser AH, Shigenaga JK, Grunfeld C, Feingold KR. The acute phase response is associated with retinoid X receptor repression in rodent liver. *J Biol Chem* 2000;275:16390–16399.
25. Zhou X, Cao L, Jiang C, Xie Y, Cheng X, Krausz KW, Qi Y, Sun L, Shah YM, Gonzalez FJ, Wang G, Hao H. PPARalpha-UGT axis activation represses intestinal FXR-FGF15 feedback signalling and exacerbates experimental colitis. *Nat Commun* 2014;5:4573.
26. Rau M, Stieger B, Monte MJ, Schmitt J, Jahn D, Frey-Wagner I, Raselli T, Marin JJ, Mullhaupt B, Rogler G, Geier A. Alterations in enterohepatic Fgf15 signaling and changes in bile acid composition depend on localization of murine intestinal inflammation. *Inflamm Bowel Dis* 2016;22:2382–2389.
27. Norkina O, Burnett TG, De Lisle RC. Bacterial overgrowth in the cystic fibrosis transmembrane conductance regulator null mouse small intestine. *Infect Immun* 2004;72:6040–6049.
28. Lynch SV, Goldfarb KC, Wild YK, Kong W, De Lisle RC, Brodie EL. Cystic fibrosis transmembrane conductance regulator knockout mice exhibit aberrant gastrointestinal microbiota. *Gut Microbes* 2013;4:41–47.
29. Norkina O, Kaur S, Ziemer D, De Lisle RC. Inflammation of the cystic fibrosis mouse small intestine. *Am J Physiol* 2004;286:G1032–G1041.
30. Sommer F, Adam N, Johansson ME, Xia L, Hansson GC, Backhed F. Altered mucus glycosylation in core 1 O-glycan-deficient mice affects microbiota composition and intestinal architecture. *PLoS One* 2014;9:e85254.
31. Goto Y, Uematsu S, Kiyono H. Epithelial glycosylation in gut homeostasis and inflammation. *Nat Immunol* 2016;17:1244–1251.
32. Thomsson KA, Hinojosa-Kurtzberg M, Axelsson KA, Domino SE, Lowe JB, Gendler SJ, Hansson GC. Intestinal mucins from cystic fibrosis mice show increased fucosylation due to an induced Fucalpha1-2 glycosyltransferase. *Biochem J* 2002;367:609–616.
33. Vanhooren V, Vandenbroucke RE, Dewaele S, Van Hamme E, Haigh JJ, Hochepped T, Libert C. Mice overexpressing beta-1,4-galactosyltransferase I are resistant to TNF-induced inflammation and DSS-induced colitis. *PLoS One* 2013;8:e79883.
34. Pickard JM, Maurice CF, Kinnebrew MA, Abt MC, Schenten D, Golovkina TV, Bogatyrev SR, Ismagilov RF, Pamer EG, Turnbaugh PJ, Chervonsky AV. Rapid

- fucosylation of intestinal epithelium sustains host-commensal symbiosis in sickness. *Nature* 2014; 514:638–641.
35. Gadaleta RM, Oldenburg B, Willemsen EC, Spit M, Murzilli S, Salvatore L, Klomp LW, Siersema PD, Van Erpecum KJ, Van Mil SW. Activation of bile salt nuclear receptor FXR is repressed by pro-inflammatory cytokines activating NF-kappaB signaling in the intestine. *Biochim Biophys Acta* 2011;1812:851–858.
  36. Huang W, Ma K, Zhang J, Qatanani M, Cuvillier J, Liu J, Dong B, Huang X, Moore DD. Nuclear receptor-dependent bile acid signaling is required for normal liver regeneration. *Science* 2006;312:233–236.
  37. Kong B, Wang L, Chiang JY, Zhang Y, Klaassen CD, Guo GL. Mechanism of tissue-specific farnesoid X receptor in suppressing the expression of genes in bile-acid synthesis in mice. *Hepatology* 2012; 56:1034–1043.
  38. Ikpa PT, Meijssen KF, Nieuwenhuijze NDA, Dulla K, De Jonge HR, Bijvelds MJC. Transcriptome analysis of the distal small intestine of Cfr null mice. *Genomics* 2019 [Epub ahead of print] <http://doi.org/10.1016/j.ygeno.2019.06.028>.
  39. Gustafsson JK, Ermund A, Ambort D, Johansson ME, Nilsson HE, Thorell K, Hebert H, Sjovall H, Hansson GC. Bicarbonate and functional CFTR channel are required for proper mucin secretion and link cystic fibrosis with its mucus phenotype. *J Exp Med* 2012;209:1263–1272.
  40. Dorsey J, Gonska T. Bacterial overgrowth, dysbiosis, inflammation, and dysmotility in the cystic fibrosis intestine. *J Cyst Fibros* 2017;16:S14–S23.
  41. Van den Bossche L, Hindryckx P, Devisscher L, Devriese S, Van Welden S, Holvoet T, Vilchez-Vargas R, Vital M, Pieper DH, Vanden Bussche J, Vanhaecke L, Van de Wiele T, De Vos M, Laukens D. Ursodeoxycholic acid and its taurine- or glycine-conjugated species reduce colitogenic dysbiosis and equally suppress experimental colitis in mice. *Appl Environ Microbiol* 2017;83 pii: e02766-16.
  42. Shukla PK, Meena AS, Rao V, Rao RG, Balazs L, Rao R. Human defensin-5 blocks ethanol and colitis-induced dysbiosis, tight junction disruption and inflammation in mouse intestine. *Sci Rep* 2018;8:16241.
  43. Liu K, Wang X, Zou C, Zhang J, Chen H, Tsang L, Yu MK, Chung YW, Wang J, Dai Y, Liu Y, Zhang X. Defective CFTR promotes intestinal proliferation via inhibition of the hedgehog pathway during cystic fibrosis. *Cancer Lett* 2019;446:15–24.
  44. Byndloss MX, Olsan EE, Rivera-Chavez F, Tiffany CR, Cevallos SA, Lokken KL, Torres TP, Byndloss AJ, Faber F, Gao Y, Litvak Y, Lopez CA, Xu G, Napoli E, Giulivi C, Tsois RM, Revzin A, Lebrilla CB, Baumler AJ. Microbiota-activated PPAR-gamma signaling inhibits dysbiotic Enterobacteriaceae expansion. *Science* 2017; 357:570–575.
  45. Harmon GS, Dumlao DS, Ng DT, Barrett KE, Dennis EA, Dong H, Glass CK. Pharmacological correction of a defect in PPAR-gamma signaling ameliorates disease severity in Cfr-deficient mice. *Nat Med* 2010; 16:313–318.
  46. Ollero M, Junaidi O, Zaman MM, Tzamelis I, Ferrando AA, Andersson C, Blanco PG, Bialecki E, Freedman SD. Decreased expression of peroxisome proliferator activated receptor gamma in cfr-/- mice. *J Cell Physiol* 2004;200:235–244.
  47. Trauner M, Boyer JL. Bile salt transporters: molecular characterization, function, and regulation. *Physiol Rev* 2003;83:633–671.
  48. Craddock AL, Love MW, Daniel RW, Kirby LC, Walters HC, Wong MH, Dawson PA. Expression and transport properties of the human ileal and renal sodium-dependent bile acid transporter. *Am J Physiol* 1998; 274:G157–G169.
  49. Sinha J, Chen F, Miloh T, Burns RC, Yu Z, Shneider BL. beta-Klotho and FGF-15/19 inhibit the apical sodium-dependent bile acid transporter in enterocytes and cholangiocytes. *Am J Physiol* 2008;295:G996–G1003.
  50. Wouthuyzen-Bakker M, Bijvelds MJC, De Jonge HR, De Lisle RC, Burgerhof JGM, Verkade HJ. Effect of antibiotic treatment on fat absorption in mice with cystic fibrosis. *Pediatr Res* 2012;71:4–12.
  51. Bodewes FA, Van der Wulp MY, Beharry S, Doktorova M, Havinga R, Boverhof R, James Phillips M, Durie PR, Verkade HJ. Altered intestinal bile salt biotransformation in a cystic fibrosis (Cfr-/-) mouse model with hepatobiliary pathology. *J Cyst Fibros* 2015;14:440–446.
  52. De Lisle RC, Roach E, Jansson K. Effects of laxative and N-acetylcysteine on mucus accumulation, bacterial load, transit, and inflammation in the cystic fibrosis mouse small intestine. *Am J Physiol* 2007;293:G577–G584.
  53. Kayama S, Mitsuyama M, Sato N, Hatakeyama K. Overgrowth and translocation of *Escherichia coli* from intestine during prolonged enteral feeding in rats. *J Gastroenterol* 2000;35:15–19.
  54. Bertolini A, Van de Peppel IP, Doktorova-Demmin M, Bodewes F, De Jonge HR, Bijvelds MJC, Verkade HJ, Jonker JW. Defective FXR-FGF15 signaling and bile acid homeostasis in cystic fibrosis mice can be restored by the laxative polyethylene glycol. *Am J Physiol* 2019; 316:G404–G411.
  55. Inagaki T, Moschetta A, Lee YK, Peng L, Zhao G, Downes M, Yu RT, Shelton JM, Richardson JA, Repa JJ, Mangelsdorf DJ, Kliewer SA. Regulation of antibacterial defense in the small intestine by the nuclear bile acid receptor. *Proc Natl Acad Sci U S A* 2006; 103:3920–3925.
  56. Wilschanski M, Rivlin J, Cohen S, Augarten A, Blau H, Aviram M, Bentur L, Springer C, Vila Y, Branski D, Kerem B, Kerem E. Clinical and genetic risk factors for cystic fibrosis-related liver disease. *Pediatrics* 1999;103:52–57.
  57. Colombo C, Battezzati PM, Crosignani A, Morabito A, Costantini D, Padoan R, Giunta A. Liver disease in cystic fibrosis: a prospective study on incidence, risk factors, and outcome. *Hepatology* 2002;36:1374–1382.
  58. Xiao F, Li J, Singh AK, Riederer B, Wang J, Sultan A, Park H, Lee MG, Lamprecht G, Scholte BJ, De Jonge HR, Seidler U. Rescue of epithelial HCO<sub>3</sub><sup>-</sup> secretion in murine intestine by apical membrane expression of the cystic fibrosis transmembrane conductance regulator mutant F508del. *J Physiol (Lond)* 2012;590:5317–5334.

59. Ikpa PT, Sleddens HFBM, Steinbrecher KA, Peppelenbosch MP, De Jonge HR, Smits R, Bijvelds MJC. Guanylin and uroguanylin are produced by mouse intestinal epithelial cells of columnar and secretory lineage. *Histochem Cell Biol* 2016;146:445–455.
60. Yang YW, Chen MK, Yang BY, Huang XJ, Zhang XR, He LQ, Zhang J, Hua ZC. Use of 16S rRNA gene-targeted group-specific primers for real-time PCR analysis of predominant bacteria in mouse feces. *Appl Environ Microbiol* 2015;81:6749–6756.
61. Mahe MM, Aihara E, Schumacher MA, Zavros Y, Montrose MH, Helmuth MA, Sato T, Shroyer NF. Establishment of gastrointestinal epithelial organoids. *Curr Protoc Mouse Biol* 2013;3:217–240.
62. Bijvelds MJC, Jorna H, Verkade HJ, Bot AGM, Hofmann F, Agellon LB, Sinaasappel M, De Jonge HR. Activation of CFTR by ASBT-mediated bile salt absorption. *Am J Physiol* 2005;289:G870–G879.
63. Van Dommelen FS, Hamer CM, De Jonge HR. Efficient entrapment of large and small compounds during vesiculation of intestinal microvilli. *Biochem J* 1986;236:771–778.
64. Torchia EC, Stolz A, Agellon LB. Differential modulation of cellular death and survival pathways by conjugated bile acids. *BMC Biochem* 2001;2:11.
65. Gerhardt KO, Gehrke CW, Rogers IT, Flynn MA, Hentges DJ. Gas-liquid chromatography of fecal neutral steroids. *J Chromatogr* 1977;135:341–349.
66. Liberzon A, Birger C, Thorvaldsdottir H, Ghandi M, Mesirov JP, Tamayo P. The Molecular Signatures Database (MSigDB) hallmark gene set collection. *Cell Syst* 2015;1:417–425.
67. Subramanian A, Tamayo P, Mootha VK, Mukherjee S, Ebert BL, Gillette MA, Paulovich A, Pomeroy SL, Golub TR, Lander ES, Mesirov JP. Gene set enrichment analysis: a knowledge-based approach for interpreting genome-wide expression profiles. *Proc Natl Acad Sci U S A* 2005;102:15545–15550.

---

Received November 17, 2017. Accepted August 16, 2019.

#### Correspondence

Address correspondence to: Marcel J. C. Bijvelds, PhD, Department of Gastroenterology and Hepatology, Erasmus MC University Medical Center, PO Box 2040, 3000CA Rotterdam, The Netherlands. e-mail: [m.bijvelds@erasmusmc.nl](mailto:m.bijvelds@erasmusmc.nl); fax: (31) 10-7032793.

#### Acknowledgments

The authors would like to thank Renze Boverhof (University Medical Center Groningen) for excellent technical assistance, and Dr Luis B. Agellon (McGill University, Montréal, Canada) for kindly donating the ASBT antibody.

#### Author contributions

Pauline T. Ikpa acquired data, analyzed and interpreted data, performed the statistical analysis, and drafted the manuscript; Marcela Doktorova acquired data, analyzed and interpreted data, and drafted the manuscript; Kelly F. Meijssen acquired data; Natascha D. A. Nieuwenhuijze acquired data; Henkjan J. Verkade was responsible for the study concept and design, critical revision of the manuscript, and obtained funding; Johan W. Jonker was responsible for the study concept and design, critical revision of the manuscript, and obtained funding; Hugo R. de Jonge was responsible for the study concept and design, critical revision of the manuscript, and obtained funding; and Marcel J. C. Bijvelds acquired data, analyzed and interpreted data, performed the statistical analysis, drafted the manuscript, and provided study supervision.

#### Conflicts of interest

The authors disclose no conflicts.

#### Funding

This study was funded by Dutch Cystic Fibrosis Foundation grant HIT-CF2, the UK Cystic Fibrosis Trust grant SRC011, Stichting Vrienden van het Beatrix Kinderziekenhuis, and the Jan Cornelis de Cock Stichting.